Time-dependent density-functional approach for exciton binding energies

V. Turkowski,[1,2] A. Leonardo,[1] and C. A. Ullrich[1]
[1]*Department of Physics and Astronomy, University of Missouri, Columbia, Missouri 65211, USA*
[2]*Department of Physics and NanoScience Technology Center, University of Central Florida, Orlando, Florida 32816, USA*
(Received 27 February 2009; revised manuscript received 22 April 2009; published 10 June 2009)

Optical processes in insulators and semiconductors, including excitonic effects, can be described in principle exactly using time-dependent density-functional theory (TDDFT). Starting from a linearization of the TDDFT semiconductor Bloch equations in a two-band model, we derive a simple formalism for calculating exciton binding energies. This formalism leads to a generalization of the standard Wannier equation for excitons, featuring a nonlocal effective electron-hole interaction determined by long-range and dynamical exchange-correlation (XC) effects. We calculate exciton binding energies in several direct-gap semiconductors using exchange-only and model XC kernels.

DOI: 10.1103/PhysRevB.79.233201 PACS number(s): 71.15.Mb, 71.35.−y, 31.15.ee

I. INTRODUCTION

The elementary model of Wannier excitons in insulators views them as bound electron-hole pairs which satisfy a hydrogenlike Schrödinger equation:[1]

$$\left[-\frac{\hbar^2\nabla^2}{2m_r}-\frac{e^2}{\epsilon r}\right]\phi(\mathbf{r})=E\phi(\mathbf{r}). \tag{1}$$

Here, m_r is the reduced electron-hole effective mass, e is the electron charge, ϵ is the static dielectric constant of the material, and ϕ and E are the excitonic wave functions and binding energies (from now on we set $\hbar=e=1$). Equation (1), also known as Wannier equation,[2] produces a Rydberg series of discrete energy states below the conduction-band edge and a redistribution of oscillator strength in the optical spectrum around the band edge which is qualitatively described by the Elliott formula.[3] Excitonic effects are important for a large variety of optical processes in organic and inorganic materials and nanoscale systems.[4,5]

Equation (1) can be derived from the semiconductor Bloch equations within the time-dependent Hartree-Fock approximation using a dielectrically screened Coulomb interaction.[3,6] It is well known that time-dependent Hartree-Fock with bare Coulomb interaction leads to very poor optical spectra of materials with strongly overbound excitons. A more rigorous *ab initio* treatment of excitation processes in insulators and semiconductors, including correlation-induced screening, can be developed using many-body Green's function techniques such as the GW/Bethe-Salpeter equation.[7]

Time-dependent density-functional theory (TDDFT) (Ref. 8) has recently emerged as an alternative, computationally convenient approach to electronic excitation processes in materials.[7,9–11] In linear-response TDDFT, excitation energies can be calculated in principle exactly,[12,13] provided the exchange-correlation (XC) kernel $f_{\rm xc}(\mathbf{r},\mathbf{r}',\omega)$ is known. In Refs. 7 and 9, an approximate $f_{\rm xc}$ was constructed from many-body Green's functions, whereas Ref. 10 uses an exact-exchange (EXX) approach, including a cutoff in wave vector space which mimics screening of the Coulomb interaction.[14] These studies have established that TDDFT is capable of accurately describing excitonic effects in solids, although one needs XC functionals that go beyond the more common ones such as the adiabatic local-density approximation (ALDA).[8] The resulting agreement with experimental data is excellent[11] but the technical effort is not significantly less than for standard many-body approaches.

The purpose of this Brief Report is to develop a formally much simpler TDDFT treatment of excitonic effects in solids. Rather than calculating complete optical spectra, our goal is more modest, namely, a method that directly yields exciton binding energies, similar to the Wannier equation (1). Starting from a TDDFT version of the semiconductor Bloch equations,[15] we derive an effective electron-hole interaction which explicitly shows how long-range XC effects are essential for exciton formation. Our simplified treatment not only provides physical insight into the way excitonic effects are treated in TDDFT but also provides a straightforward way of testing approximate XC functionals.

II. TIME-DEPENDENT KOHN-SHAM FORMALISM FOR SOLIDS

In TDDFT, the electron dynamics of a solid is described by the time-dependent Kohn-Sham (KS) orbitals $\Psi_{j\mathbf{k}}(\mathbf{r},t)$, where $\mathbf{k}$ is the wave vector and j is the valence-band index (only the time evolution of the initially occupied states is considered). The system is assumed to start from the ground state, $\Psi_{j\mathbf{k}}(\mathbf{r},t_0)=\psi_{j\mathbf{k}}(\mathbf{r})$. The KS Bloch functions and band structure follow from

$$\left[-\frac{\nabla^2}{2m}+V_{\rm lat}(\mathbf{r})+V_{\rm H}^0(\mathbf{r})+V_{\rm xc}^0(\mathbf{r})-\varepsilon_{j\mathbf{k}}\right]\psi_{j\mathbf{k}}(\mathbf{r})=0, \tag{2}$$

where $V_{\rm lat}$ is the crystal lattice potential (within the Born-Oppenheimer approximation) and $V_{\rm H}^0$ and $V_{\rm xc}^0$ are the static Hartree and XC potentials.

Since the $\psi_{j\mathbf{k}}(\mathbf{r})$ form a complete set for each $\mathbf{k}$, we can expand the time-dependent KS orbitals as follows:

$$\Psi_{j\mathbf{k}}(\mathbf{r},t)=\sum_l c_{\mathbf{k}}^{jl}(t)\psi_{l\mathbf{k}}(\mathbf{r}), \tag{3}$$

where the summation runs over all valence and conduction bands, including continuum states. Equation (3) is appropriate if we assume the system to interact with an electromag-

netic field in dipole approximation. We define the density matrix $\rho_{j\mathbf{k}}^{lm}(t)=c_{\mathbf{k}}^{jl}(t)[c_{\mathbf{k}}^{jm}(t)]^*$, whose equation of motion is

$$i\frac{\partial}{\partial t}\boldsymbol{\rho}_{j\mathbf{k}}(t)=[\mathbf{H}_{\mathbf{k}}(t),\boldsymbol{\rho}_{j\mathbf{k}}(t)], \tag{4}$$

with initial condition $\rho_{j\mathbf{k}}^{lm}(t_0)=\delta_{jl}\delta_{ml}$. The matrix elements of the TDDFT Hamiltonian are

$$H_{\mathbf{k}}^{lm}(t)=\frac{1}{\Omega}\int_{\Omega}d^3r\psi_{l\mathbf{k}}^*(\mathbf{r})H(t)\psi_{m\mathbf{k}}(\mathbf{r})$$

$$=\varepsilon_{l\mathbf{k}}\delta_{lm}+\mathbf{E}(t)\mathbf{d}_{\mathbf{k}}^{lm}+\tilde{V}_{\mathrm{H}\mathbf{k}}^{lm}(t)+\tilde{V}_{\mathrm{xc}\mathbf{k}}^{lm}(t), \tag{5}$$

where Ω is the volume of the lattice unit cell, $\mathbf{E}(t)$ is the electric-field amplitude, and $\mathbf{d}_{\mathbf{k}}^{lm}$ are the dipole matrix elements. $\tilde{V}_{\mathrm{H}}(t)=V_{\mathrm{H}}(t)-V_{\mathrm{H}}^0$ denotes the dynamic part of the Hartree potential, and similar for XC. Self-consistent solution of Eq. (4), with the time-dependent density

$$n(\mathbf{r},t)=2\sum_{j\mathbf{k}}\theta(\varepsilon_F-\varepsilon_{j\mathbf{k}})\sum_{lm}\rho_{j\mathbf{k}}^{lm}(t)\psi_{l\mathbf{k}}(\mathbf{r})\psi_{m\mathbf{k}}^*(\mathbf{r}), \tag{6}$$

where ε_F is the Fermi energy, is equivalent to solving the time-dependent KS equations for the solid, and is thus in principle exact.

III. TWO-BAND MODEL AND EXCITONS

To study optical excitation processes near the band gap, a two-band model is a reasonable and widely used approximation. We consider one valence and one conduction band, v and c, assumed to be nondegenerate (see Ref. 16 for a discussion of band degeneracy). The index j of the density matrix $\rho_{j\mathbf{k}}^{lm}(t)$ refers to v and will be dropped in the following. Equation (4) yields the TDDFT semiconductor Bloch equations for the two independent components $\rho_{\mathbf{k}}^{vv}$ and $\rho_{\mathbf{k}}^{vc}$,[15]

$$\frac{\partial}{\partial t}\rho_{\mathbf{k}}^{vv}(t)=-2\,\mathrm{Im}\{[\mathbf{E}(t)\mathbf{d}_{\mathbf{k}}^{cv}+\tilde{V}_{\mathrm{H}\mathbf{k}}^{cv}(t)+\tilde{V}_{\mathrm{xc}\mathbf{k}}^{cv}(t)]\rho_{\mathbf{k}}^{vc}(t)\}, \tag{7}$$

$$i\frac{\partial}{\partial t}\rho_{\mathbf{k}}^{vc}(t)=[\varepsilon_{\mathbf{k}}^{v}-\varepsilon_{\mathbf{k}}^{c}+\tilde{V}_{\mathrm{H}\mathbf{k}}^{vv}(t)+\tilde{V}_{\mathrm{xc}\mathbf{k}}^{vv}(t)-\tilde{V}_{\mathrm{H}\mathbf{k}}^{cc}(t)$$

$$-\tilde{V}_{\mathrm{xc}\mathbf{k}}^{cc}(t)]\rho_{\mathbf{k}}^{vc}(t)+[\mathbf{E}(t)\mathbf{d}_{\mathbf{k}}^{vc}+\tilde{V}_{\mathrm{H}\mathbf{k}}^{vc}(t)+\tilde{V}_{\mathrm{xc}\mathbf{k}}^{vc}(t)]$$

$$\times[\rho_{\mathbf{k}}^{cc}(t)-\rho_{\mathbf{k}}^{vv}(t)]. \tag{8}$$

Notice that $\rho_{\mathbf{k}}^{vv}+\rho_{\mathbf{k}}^{cc}=1$ and $\rho_{\mathbf{k}}^{vc}=\rho_{\mathbf{k}}^{cv*}$. In Ref. 15, Eqs. (7) and (8) were evaluated in the time domain for ultrafast pulsed excitations. Here, we are interested in exciton binding energies and we linearize Eq. (8):

$$i\frac{\partial}{\partial t}\rho_{\mathbf{k}}^{vc}(t)=[\varepsilon_{\mathbf{k}}^{v}-\varepsilon_{\mathbf{k}}^{c}]\rho_{\mathbf{k}}^{vc}(t)-\delta\tilde{V}_{\mathrm{H}\mathbf{k}}^{vc}(t)-\delta\tilde{V}_{\mathrm{xc}\mathbf{k}}^{vc}(t), \tag{9}$$

where we dropped the time-dependent external field term since the excitations we are interested in can be viewed as eigenmodes of the system. Here, $\delta\tilde{V}_{\mathrm{H}\mathbf{k}}^{vc}$ and $\delta\tilde{V}_{\mathrm{xc}\mathbf{k}}^{vc}$ denote the linearized dynamical Hartree and XC potentials. In a periodic insulating solid, the Hartree term only gives rise to the so-called local-field corrections, which do not affect excitonic binding.[7] We will therefore only keep the XC contribution in the following.

Fourier transformation of Eq. (9) and the corresponding equation for $\rho_{\mathbf{k}}^{cv}(t)$ leads to

$$\rho_{\mathbf{k}}^{vc}(\omega)=-\frac{\sum_{\mathbf{q}}[F_{\mathbf{kq}}^{vcvc}(\omega)\rho_{\mathbf{q}}^{vc}(\omega)+F_{\mathbf{kq}}^{vcvc}(\omega)\rho_{\mathbf{q}}^{cv}(\omega)]}{\omega+\omega_{\mathbf{k}}^{cv}}, \tag{10}$$

$$\rho_{\mathbf{k}}^{cv}(\omega)=\frac{\sum_{\mathbf{q}}[F_{\mathbf{kq}}^{cvcv}(\omega)\rho_{\mathbf{q}}^{vc}(\omega)+F_{\mathbf{kq}}^{cvvc}(\omega)\rho_{\mathbf{q}}^{cv}(\omega)]}{\omega-\omega_{\mathbf{k}}^{cv}}, \tag{11}$$

where $\omega_{\mathbf{k}}^{cv}=\varepsilon_{\mathbf{k}}^{c}-\varepsilon_{\mathbf{k}}^{v}$,

$$F_{\mathbf{kq}}^{ijmn}(\omega)=\frac{2}{\Omega^2}\int_{\Omega}d^3r\int_{\Omega}d^3r'\psi_{i\mathbf{k}}^*(\mathbf{r})\psi_{j\mathbf{k}}(\mathbf{r})f_{\mathrm{xc}}(\mathbf{r},\mathbf{r}',\omega)$$

$$\times\psi_{m\mathbf{q}}^*(\mathbf{r}')\psi_{n\mathbf{q}}(\mathbf{r}'), \tag{12}$$

and the $\mathbf{q}$ summation runs over the first Brillouin zone. Equations (10) and (11) can be cast into an eigenvalue problem for the excitation energies ω. Since f_{xc} is in general frequency dependent, the eigenvalue problem is nonlinear. The solutions are the exact exciton binding energies within the two-band model.

Let us carry out a further simplification. Since typical exciton binding energies are much smaller than the band gap, i.e., $\omega+\omega_{\mathbf{k}}^{cv}\gg\omega-\omega_{\mathbf{k}}^{cv}$, we can ignore the pole at negative ω (which is equivalent to the Tamm-Dancoff approximation[8]) and boldly set $\rho_{\mathbf{k}}^{vc}=0$. This leads to

$$\sum_{\mathbf{q}}[\omega_{\mathbf{q}}^{cv}\delta_{\mathbf{kq}}+F_{\mathbf{kq}}^{cvvc}(\omega)]\rho_{\mathbf{q}}^{cv}(\omega)=\omega\rho_{\mathbf{k}}^{cv}(\omega). \tag{13}$$

Equation (13) is the equivalent for extended systems of the well-known single-pole approximation of linear-response TDDFT.[12] For finite atomic or molecular systems, the single-pole approximation only involves two discrete levels. Here, it involves two entire bands, which clearly shows the collective nature of excitonic effects. We point out that Eq. (13) yields exciton binding energies relative to the conduction-band edge, which can be accurate even if the band gap itself is not.

IV. TDDFT WANNIER EQUATION

Our next goal is to derive a real-space equation for the exciton binding energies. $\rho_{\mathbf{k}}^{cv}$ is a periodic function in reciprocal space, with Fourier transform $\rho(\mathbf{R},\omega)=\Sigma_{\mathbf{k}}e^{-i\mathbf{k}\cdot\mathbf{R}}\rho_{\mathbf{k}}^{cv}(\omega)$, where $\mathbf{R}$ is a direct lattice vector. Similarly, we define

$$V_{eh}(\mathbf{R},\mathbf{R}',\omega)=\sum_{\mathbf{k},\mathbf{q}}e^{-i\mathbf{k}\cdot\mathbf{R}}F_{\mathbf{kq}}^{cvvc}(\omega)e^{i\mathbf{q}\cdot\mathbf{R}'}. \tag{14}$$

From the point of view of a Wannier exciton, which extends over many lattice constants, $\mathbf{R}$ can be approximated as a continuous variable. We assume a direct band-gap material and use approximate parabolic dispersions with conduction- and valence-band effective masses m_c and m_v, and reduced electron-hole effective mass $m_r^{-1}=m_c^{-1}+m_v^{-1}$. This yields the TDDFT version of the Wannier equation (1),

$$\left[-\frac{\nabla^2}{2m_r}-E_{b,i}\right]\rho_i(\mathbf{r})+\int_{\substack{\text{all}\\ \text{space}}} d^3r' V_{eh}(\mathbf{r},\mathbf{r}',\omega)\rho_i(\mathbf{r}')=0, \tag{15}$$

featuring a nonlocal, frequency-dependent electron-hole interaction $V_{eh}(\mathbf{r},\mathbf{r}',\omega)$, where $\omega=E_g^{\mathrm{KS}}+E_{b,i}$, and E_g^{KS} is the KS band gap. The ith exciton binding energy $E_{b,i}$ is measured with respect to the KS conduction-band edge and the $\rho_i(\mathbf{r})$ are the analog of the excitonic wave functions $\phi(\mathbf{r})$ of Eq. (1).

V. XC KERNELS

The effective electron-hole interaction in TDDFT and thus the exciton binding energies depend crucially on the approximate XC kernel. In the following, we shall implement several simple frequency-independent XC kernels and test their performance in our formalism.

The exchange-only ALDA kernel is given by

$$f_{\mathrm{x}}^{\mathrm{ALDA}}(\mathbf{r},\mathbf{r}')=-[9\pi n_0^2(\mathbf{r})]^{-1/3}\delta(\mathbf{r}-\mathbf{r}'), \tag{16}$$

where $n_0(\mathbf{r})$ is the equilibrium electron density. $f_{\mathrm{x}}^{\mathrm{ALDA}}$ belongs to the class of ultra-short-range kernels; the simplest of them is

$$f_{\mathrm{xc}}^{\mathrm{contact}}(\mathbf{r},\mathbf{r}')=-A\,\delta(\mathbf{r}-\mathbf{r}'), \tag{17}$$

where A is a positive constant. Such kernels have been used with some success in contact exciton models.[11]

An approximation of EXX TDDFT,[10] the Slater exchange kernel, is given by[12]

$$f_{\mathrm{x}}^{\mathrm{Slater}}(\mathbf{r},\mathbf{r}')=-\frac{2\left|\sum_{j\mathbf{k}}\theta(\epsilon_F-\epsilon_{j\mathbf{k}})\psi_{j\mathbf{k}}(\mathbf{r})\psi_{j\mathbf{k}}^*(\mathbf{r}')\right|^2}{|\mathbf{r}-\mathbf{r}'|n_0(\mathbf{r})n_0(\mathbf{r}')}. \tag{18}$$

This kernel exhibits some degree of long-range behavior[17] but not the ultranonlocality ($\sim 1/q^2$ in momentum space) of the exact f_{xc}.[7,10,11] This long-range contribution (LRC) can be explicitly taken into account using the following model kernel:[18]

$$f_{\mathrm{xc}}^{\mathrm{LRC}}(\mathbf{r},\mathbf{r}')=-\frac{\alpha}{4\pi|\mathbf{r}-\mathbf{r}'|}, \tag{19}$$

where α is again an adjustable parameter.

VI. RESULTS AND DISCUSSION

We have tested our TDDFT approach for exciton binding energies, Eq. (13), for the zinc-blende materials GaAs and β-GaN and for the wurtzite materials α-GaN, CdS, and CdSe. The Bloch functions for the conduction and heavy-hole valence bands were obtained from local-density approximation (LDA) band structures calculated with the plane-wave pseudopotential code ABINIT.[19] We used on the order of 500 **k** points in the first Brillouin zone for all materials. Out of these, there are ten independent points for GaAs and β-GaN and 20 for α-GaN, CdS, and CdSe, which determines the dimension of the eigenvalue problem (13). Recent Bethe-Salpeter calculations of exciton binding energies used much higher **k**-point densities close to the zone center;[20,21] we performed convergence checks of our **k**-point sampling rates and found them to be sufficiently accurate for our simple model.

TABLE I. E_b^{exp} and E_b^{Slater}: lowest direct exciton binding energies (in meV) for selected III-V and II-VI compounds, from experiment (Ref. 22) and from Eqs. (13) and (12) with $f_{\mathrm{x}}^{\mathrm{Slater}}$. The parameters A and $\alpha/4\pi$ (in a.u.) are fitted to reproduce E_b^{exp} using Eqs. (13) and (12) with $f_{\mathrm{xc}}^{\mathrm{contact}}$ and $f_{\mathrm{xc}}^{\mathrm{LRC}}$.

	A	$\alpha/4\pi$	E_b^{Slater}	E_b^{exp}
GaAs	0.42	0.12	17.8	3.27
β-GaN	1.06	0.55	28.7	26.0
α-GaN	2.03	0.91	11.8	20.4
CdS	6.28	1.83	7.9	28.0
CdSe	4.84	1.19	8.3	15.0

As expected, the ALDA does not produce any bound excitons. Results for the other three XC kernels and experimental binding energies of the lowest direct excitons are presented in Table I. The contact and LRC kernels, Eqs. (17) and (19), contain adjustable parameters which can be tuned to reproduce the experimental exciton binding energies. In Ref. 18, $\alpha/4\pi=0.2$ was found for GaAs, which is similar to our results in Table I. In Ref. 23, $A=15$ was obtained for Si, which is somewhat larger than our values of A for III-V and II-VI materials.

The contact and LRC kernels only yield a single excitonic bound state.[18] This is generally the case for static XC kernels that are local in reciprocal space, i.e., have the form $f_{\mathrm{xc}}(\mathbf{q})$. The Slater XC kernel [Eq. (18)] does have some degree of nonlocality in reciprocal space but we found that it only produces a single excitonic state, like the local kernels. To obtain an excitonic Rydberg series one needs an XC kernel that has a sufficiently strong nonlocal form or is frequency dependent.[23,24]

Looking at the results obtained with $f_{\mathrm{x}}^{\mathrm{Slater}}$, we find excitons that are overbound by 14 meV in GaAs and by 2.7 meV in β-GaN. This overbinding is what one would expect from an unscreened exchange-only approach (electronic screening can be viewed as a correlation effect). On the other hand, $f_{\mathrm{x}}^{\mathrm{Slater}}$ approaches a constant for $q\to 0$ in homogeneous systems,[17] whereas the full EXX f_{x} behaves as $1/q^2$.[10] This would suggest that $f_{\mathrm{x}}^{\mathrm{Slater}}$ has a somewhat weaker effective electron-hole interaction than full EXX. This trend seems confirmed in the wurtzite materials whose calculated exciton binding energies are significantly below experiment.

Additional insight is provided by comparing the electron-hole interaction V_{eh} for the different XC kernels under study. Figure 1 shows $V_{eh}(\mathbf{r},0)$ for GaAs along the x direction (due to the finite sampling in **k** space, V_{eh} can only be reliably calculated within the range of about one unit cell). In ALDA, the interaction is close to zero and thus too shallow to lead to any excitonic binding. The other XC kernels produce stronger electron-hole interactions, where for GaAs the contact and LRC models are less attractive than the Slater approximation.

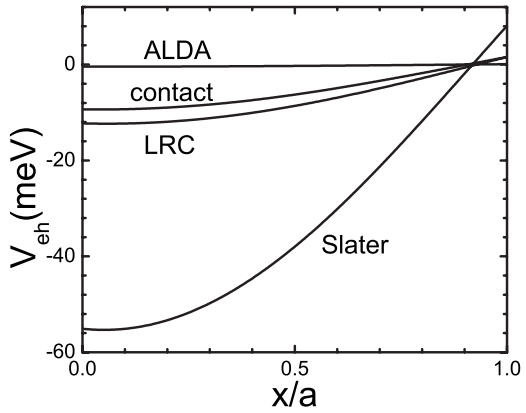

FIG. 1. Effective electron-hole interaction $V_{eh}(\mathbf{r},0)$ for GaAs and different XC kernels plotted along the x direction, where a is the lattice constant. The parameters A and α for the contact and the LRC XC kernels are given in Table I.

VII. CONCLUSION

We have presented a simple method to calculate exciton binding energies using TDDFT. The main idea, restricting the dynamics to the highest valence and the lowest conduction band, is similar to the single-pole approximation for excitation energies.[12] Our derivation was based on the TDDFT semiconductor Bloch equation; an alternative starting point could be the Casida formalism of linear-response TDDFT,[13] formulated for periodic systems.[25] The resulting simple eigenvalue equation in momentum space, Eq. (13), is readily diagonalized to yield the exciton binding energies. Transformation into real space leads to the TDDFT analog of the Wannier equation for excitons and shows that the effective electron-hole interaction is nonlocal.

The quality of the results depends crucially on the approximation used for $f_{\mathrm{xc}}(\mathbf{r},\mathbf{r}',\omega)$. It is well known that local and semilocal approximations such as the ALDA do not produce any excitons. There exist sophisticated parameter-free XC kernels[9] that are capable of reproducing experimental optical-absorption spectra very accurately, including bound excitons,[24] but with substantial computational cost.

If only particular aspects of the optical spectrum of a material are required such as, for instance, the lowest bound exciton, simple static XC kernels can be a convenient alternative. The contact and the LRC kernels behave quite similarly in the sense that they produce a single excitonic peak. A detailed analysis was given in Ref. 23 and we find the same behavior in our two-band approach. The parameter-free Slater exchange-only kernel also produces a single exciton, which was found to be overbound in zinc-blende materials, and underbound in wurtzite. There are theoretical arguments in favor of both trends, which suggests a need for more systematic studies of the Slater exchange kernel in solids.

In conclusion, our simple approach for exciton binding energies is a promising method to test XC kernels in solids. It can be extended in a straightforward way to deal with spin-dependent excitations (triplet excitons), to implement more sophisticated XC kernels, or to include more bands. Furthermore, the model can be easily made time dependent to study ultrafast nonlinear excitations using the TDDFT semiconductor Bloch equations.

ACKNOWLEDGMENTS

This work was supported by Research Corporation and by NSF under Grant No. DMR-0553485. We thank Angel Rubio, Lucia Reining, and Claudia Ambrosch-Draxl for useful discussions.

[1] M. P. Marder, *Condensed Matter Physics* (Wiley, New York, 2000).
[2] G. H. Wannier, Phys. Rev. **52**, 191 (1937).
[3] H. Haug and S. W. Koch, *Quantum Theory of the Optical and Electronic Properties of Semiconductors*, 4th ed. (World Scientific, Singapore, 2004).
[4] S. W. Koch *et al.*, Nature Mater. **5**, 523 (2006).
[5] G. D. Scholes and G. Rumbles, Nature Mater. **5**, 683 (2006).
[6] W. Schäfer and M. Wegener, *Semiconductor Optics and Transport Phenomena* (Springer, Berlin, 2002).
[7] G. Onida *et al.*, Rev. Mod. Phys. **74**, 601 (2002).
[8] *Time-Dependent Density-Functional Theory*, edited by M. A. L. Marques *et al.*, Lecture Notes in Physics Vol. 706 (Springer, Berlin, 2006).
[9] L. Reining *et al.*, Phys. Rev. Lett. **88**, 066404 (2002); A. Marini *et al.*, *ibid.* **91**, 256402 (2003).
[10] Y. H. Kim and A. Görling, Phys. Rev. Lett. **89**, 096402 (2002); Phys. Rev. B **66**, 035114 (2002).
[11] S. Botti *et al.*, Rep. Prog. Phys. **70**, 357 (2007).
[12] M. Petersilka *et al.*, Phys. Rev. Lett. **76**, 1212 (1996).
[13] M. E. Casida, in *Recent Advances in Density-Functional Methods*, edited by D. E. Chong (World Scientific, Singapore, 1995), Vol. 1, p. 155.
[14] F. Bruneval *et al.*, J. Chem. Phys. **124**, 144113 (2006).
[15] V. Turkowski and C. A. Ullrich, Phys. Rev. B **77**, 075204 (2008).
[16] A. Baldereschi and N. C. Lipari, Phys. Rev. B **3**, 439 (1971).
[17] M. Lein *et al.*, Phys. Rev. B **61**, 13431 (2000).
[18] S. Botti *et al.*, Phys. Rev. B **69**, 155112 (2004).
[19] X. Gonze *et al.*, Comput. Mater. Sci. **25**, 478 (2002); X. Gonze, Z. Kristallogr. **220**, 558 (2005).
[20] R. Laskowski *et al.*, Phys. Rev. B **72**, 035204 (2005).
[21] F. Fuchs *et al.*, Phys. Rev. B **78**, 085103 (2008).
[22] P. Parenteau *et al.*, J. Appl. Phys. **71**, 3747 (1992), GaAs; D. J. As *et al.*, Appl. Phys. Lett. **70**, 1311 (1997), $\beta-$GaN; J. F. Muth *et al.*, *ibid.* **71**, 2572 (1997), $\alpha-$GaN; M. A. Jakobson *et al.*, J. Cryst. Growth **138**, 225 (1994), CdS; J. Voigt *et al.*, Phys. Status Solidi B **91**, 189 (1979), CdSe.
[23] F. Sottile *et al.*, Phys. Rev. B **68**, 205112 (2003).
[24] F. Sottile *et al.*, Phys. Rev. B **76**, 161103(R) (2007).
[25] M. Grüning and X. Gonze, Phys. Rev. B **76**, 035126 (2007).